Microwave Radar for Breast Health Monitoring: System Performance Protocol

Lena Kranold
Department of Electrical and Computer Engineering
McGill Univeristy
Montreal, Canada
lena.kranold@mail.mcgill.ca

Muberra Ozmen
Department of Electrical and Computer Engineering
McGill Univeristy
Montreal, Canada
muberra.ozmen@mail.mcgill.ca

Mark Coates
Department of Electrical and Computer Engineering
McGill Univeristy
Montreal, Canada
mark.coates@mcgill.ca

Milica Popović
Department of Electrical and Computer Engineering
McGill Univeristy
Montreal, Canada
milica.popovich@mcgill.ca

***Abstract*— We here report on a protocol of system performance for the microwave radar breast health monitoring prototype. The device aims to detect breast cancer at an early stage and operates in the multistatic mode with 16 transceiving antennas. After introducing hardware changes, we developed a system performance protocol to repeatably test our system in preparation for clinical trials. It includes repeated scans using breast phantoms, and we investigated if the phantoms can be used without a matching medium not only with an ideally-fitting antenna housing, but also with the prosthetic bra used in clinical trials. We compare the system performance of with both antenna housing options and introduce a system performance protocol for the clinical trials.**

***Keywords*— microwave imaging, antennas, measurements**

I. Introduction

According to the American Cancer Society [1], the second most common cause of death by cancer in women is breast cancer. Recent statistics show that the stage 1 5-year survival rate is 99 %, as opposed to stage 4 with only 27 %. Hence, the earlier the diagnosis is done, the higher the chances are for the patient survival. The current screening technologies, such as X-ray mammography, MRI and ultrasound, have drawbacks, e. g. ionizing radiation, expensive operational costs, or invasiveness. Microwave technologies are currently investigated by different research groups as a promising alternative technology that aims to avoid those common drawbacks [2]. They are non-invasive, apply non-ionizing radiation, and available at a low cost. Different prototypes in [3-5] use the microwave radar (MWR) and have been tested for suitability as a screening modality on experimental breast models as well as volunteers.

Our multistatic MWR system operates at 2 – 4 GHz and has been tested on patients [5]. For further clinical trials, it is important to ensure proper operation of the system at the start and end of each trial day. Hence, a system performance protocol was developed and tested for repeatability purposes. We designed a robust protocol to test our system with experimental breast models, using an antenna housing that is best suited for the phantoms. Then, we investigated if the same protocol can be used on the antenna housing designed for patient scans. Finally, we propose a set of experimental scans to be performed before and after each patient scan and investigated two different data analysis methods to evaluate the system performance.

This work was supported by the following grants of the Natural Sciences and Engineering Research Council of Canada (NSERC): Discovery (NSERC RGPIN-2019-05850) and Collaborative Research and Development (CRDPJ 521870 – 17, with Analog Devices, Inc).

II. Materials and Methods

A. System Setup

The experimental system (Fig. 1) has a clock that is triggering a Gaussian pulse generator and a digital oscilloscope. The pulse is then shaped to have its main content in the range 2 – 4 GHz. The switching circuit sets one of the 16 rectangular patch antennas from [6] into transmitting and another into receiving mode, switching through 240 multistatic antenna pairs one at a time. The digital sampling oscilloscope records the signals at 160 GSa/s and takes 16 averages per sample. The 16 antennas are housed in either a 3D-printed hemisphere, shown in Fig. 2 (a), which makes a perfect fit for the tissue phantoms, or in a prosthetic bra, Fig. 2 (b), which is better suited for the measurements on volunteers The antennas in the hemisphere and in the prosthetic bra have slightly different distribution to optimize the coverage of the two different surfaces.

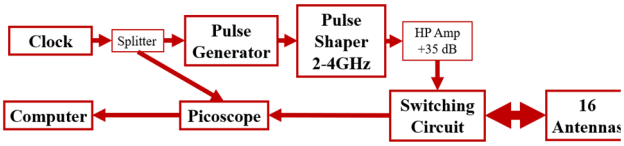

Fig. 1. System layout.

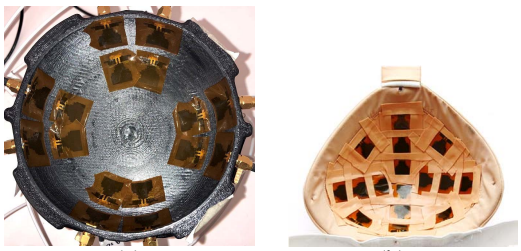

(a) (b)

Fig. 2. (a) 3D printed hemisphere housing 16 flexible patch antennas and (b) prosthetic bra housing 16 flexible patch antennas.

978-1-7281-5866-2/20/$31.00 ©2020 Crown

B. Experimental Breast Models

We test the functionality of the MWR system with a stable dispersive breast phantom consisting of a carbon-rubber mixture following the method in [7]. The hemispherical phantoms have a cylindrical gap, in which interchangeable plugs have an air-tight fit. The plugs mimic different cases: A healthy plug consists of the same fat-mimicking material as the rest of the phantom, while a tumorous plug includes a 1 cm diameter tumor, as illustrated in Fig. 3. In this study, one phantom consisting of homogeneous fat-mimicking material with no skin layer was used, referred to as Phantom A (electrical permittivity $\varepsilon_r = 8$ at center frequency, 3 GHz), with a healthy plug to imitate baseline scans and a tumorous (ε_r (3 GHz) = 60) plug to imitate tumorous scans. Furthermore, we used a second phantom with a homogeneous fat-mimicking interior (ε_r (3 GHz) = 11) and a 2.5-mm thick skin layer (ε_r (3 GHz) = 35), Phantom B. The tumor location for Phantom A is approximately 2.8 cm from the origin of the hemisphere at a depth of 3.3 cm (from the chest wall, flat surface of the phantom). For phantom B, the tumor lies at a depth of 3.0 cm and approximately 2.9 cm from the origin.

C. Methods

To evaluate the proper performance of the system before a patient or volunteer is scanned, we introduce a system performance protocol. This consists of two consecutive Baseline scans with a phantom, followed by two Tumor scans. We first evaluate the system performance using phantom scans with the 3D printed hemisphere on the homogeneous Phantom A, and compare these scans to scans performed with the prosthetic bra on Phantom A. In addition, the system with the prosthetic bra is tested on a phantom including a skin layer, Phantom B.

The results are analyzed with two separate methods. The first is based on the simple comparison of the signals of healthy scans with the signals of tumorous scans. The underlying hypothesis is that the mean energy of the signal differences between two scans of the same nature (Baseline vs. Baseline or Tumor vs. Tumor) is significantly smaller than the mean energy of the signal differences between two scans of different nature (Baseline vs. Tumor scans). The mean energy of the signal differences is calculated by subtracting each antenna pair signal of one scan from the corresponding signal of another scan, calculating the energy of each resultant difference signal, and then calculating the mean over these 240 energy values. If the 95 % confidence interval around the mean energy of the signal differences in a same case comparison is smaller and does not overlap with the 95 % confidence interval around the mean of the different case comparison, the tumor detection based on this simple test is considered successful.

(a) (b) (c)

Fig. 3. Carbon-rubber phantom (a) with hole to insert different plugs (b). (c) Schematic of tumorous plug.

We further analyze the scans using the delay-multiply-and-sum-algorithm (DMAS) from [8], which calculates a 3-D image of the scatterers within the breast. With the DMAS, we determine the signal-to-clutter-ratio (SCR), signal-to-mean-ratio (SMR) and localization error (loc. error). The SCR (dB) is the ratio of the maximum scatterer at the known tumor location in the phantom to the next highest maximum scatterer outside a 3 cm × 3 cm × 3 cm box around the tumor center. A positive SCR reflects successful tumor detection while a negative SCR means the detection failed. The SMR compares the maximum scatterer at the known tumor location to the mean scattering in the 3-D volume and is an index for contrast. The localization error is the absolute distance of the maximum scatterer in the 3-D volume to the center of the known tumor location.

III. Results

All DMAS images shown in this report refer with the z-axis from the center of the chest wall (origin of hemisphere) towards the nipple. The images are normalized to the maximum scatterer within the 3D volume, hence dark red represents a value of 1, and dark blue 0. The red *"x"* marks the x-y-coordinates of the tumor center.

A. Phantom A: Homogeneous Fat

With Phantom A as the subject, Tables I and II summarize the results of the mean energy of the signal differences for the scans recorded with the 3D printed hemisphere and with the prosthetic bra, respectively. We observe that the confidence intervals for same-case comparisons are not overlapping with the confidence intervals for Baseline-Tumor comparisons.

TABLE I. Mean, Standard Deviation and Confidence Interval for Phantom A with 3D Printed Hemisphere Housing.

Comparison	Mean	Standard deviation	95 % Confidence interval
Baseline1-Baseline2	0.0002	0.0003	[0.0001;0.0002]
Tumor1-Tumor2	0.0002	0.0002	[0.0001;0.0002]
Baseline1-Tumor1	0.0030	0.0090	[0.0019;0.0042]
Baseline1-Tumor2	0.0031	0.0090	[0.0019;0.0042]
Baseline2-Tumor1	0.0030	0.0090	[0.0018;0.0041]
Baseline2-Tumor2	0.0030	0.0091	[0.0018;0.0041]

TABLE II. Mean, Standard Deviation and Confidence Interval for Phantom A with Prosthetic Bra Housing.

Comparison	Mean	Standard deviation	95 % Confidence interval
Baseline1-Baseline2	0.0003	0.0010	[0.0002;0.0004]
Tumor1-Tumor2	0.0002	0.0005	[0.0002;0.0003]
Baseline1-Tumor1	0.0027	0.0067	[0.0019;0.0036]
Baseline1-Tumor2	0.0028	0.0067	[0.0019;0.0036]
Baseline2-Tumor1	0.0027	0.0064	[0.0019;0.0035]
Baseline2-Tumor2	0.0027	0.0063	[0.0019;0.0035]

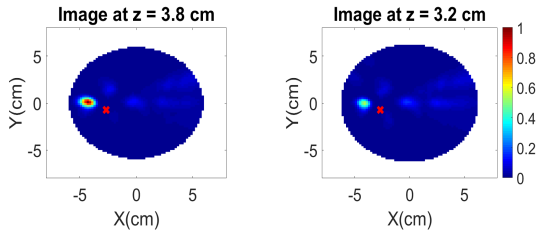

(a) (b)

Fig. 4. DMAS image with 3D printed hemisphere for Phantom A: (a) maximum scatterer slice and (b) tumor depth slice.

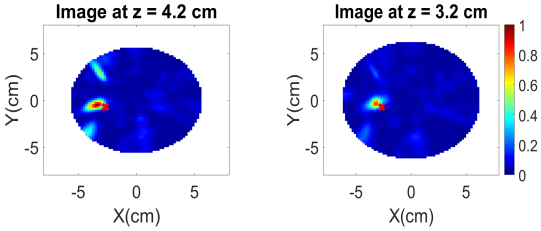

(a) (b)

Fig. 5. DMAS image with prosthetic bra for Phantom A: (a) maximum scatterer slice and (b) tumor depth slice.

The DMAS images for Phantom A are shown in Fig. 4 for the 3D printed hemisphere housing and in Fig. 5 for the prosthetic bra, with quantitative result shown in Tab. III.

We notice that the DMAS image for the ideally fitting 3D printed hemisphere show no artifacts apart from the main scattering tumor, and results in a high SMR of 45.5 dB and a positive SCR of 1.4 dB. The localization error is 2.0 cm and hence the tumor is detected in the correct region. The scans with the prosthetic bra still show the main scatterer in the tumor region, but with artifacts of increased scattering visible. However, the positive SCR = 1.3 dB and a localization error is only 1.2 cm. The tumor detection is successful using the prosthetic bra on the hemispherical phantom as well.

TABLE III. SMR, SCR, LOCALIZATION ERROR FOR PHANTOM A WITH 3D PRINTED HEMISPHERE HOUSING AND PROSTHETIC BRA HOUSING.

Housing	SCR	SMR	Localization error
3D printed hemisphere	1.4 dB	45.5 dB	2.0 cm
Prosthetic bra	1.3 dB	30.4 dB	1.2 cm

B. Phantom B: Homogeneous Fat with Skin Layer

Results for Phantom B recorded with the prosthetic bra are displayed in Tab. IV. Observing the lower edge of the confidence interval of Baseline-Tumor comparisons and the higher edge of same-case comparisons, we see that the simple method can differentiate the Baseline from the Tumor scans.

The DMAS image (here not shown due to space constraints), of the maximum scatterer slice shows that the maximum scatterer is not at the tumor location. The SCR reflects this failed detection with -6.1 dB. Therefore, for the phantom with skin, the mean energy of the signal differences algorithm proves to be more robust than the DMAS, and is suitable for a system evaluation before clinical trials.

TABLE IV. MEAN, STANDARD DEVIATION AND CONFIDENCE INTERVAL FOR PHANTOM B WITH PROSTHETIC BRA HOUSING.

Comparison	Mean	Standard deviation	95 % Confidence interval
Baseline1-Baseline2	0.0005	0.0018	[0.0003;0.0008]
Tumor1-Tumor2	0.0003	0.0006	[0.0002;0.0004]
Baseline1-Tumor1	0.0475	0.1912	[0.0232;0.0719]
Baseline1-Tumor2	0.0462	0.1899	[0.0220;0.0703]
Baseline2-Tumor1	0.0464	0.1874	[0.0226;0.0702]
Baseline2-Tumor2	0.0454	0.1864	[0.0217;0.0691]

TABLE V. SMR, SCR, LOCALIZATION ERROR FOR PHANTOM B WITH PROSTHETIC BRA HOUSING.

Housing	SCR	SMR	Localization error
Prosthetic bra	-6.1 dB	19.2 dB	8.3 cm

IV. CONCLUSION

We presented a system performance protocol for routine use in clinical trials to ensure proper system functioning. We compared a 3-D printed antenna housing with the prosthetic bra and showed that the hemispherical phantoms can successfully be scanned with the prosthetic bra without a matching medium. This implies ensured repeatability of the experiments. We intend to validate the system through these tests with selected breast phantoms on each clinical trial day. We then analyze the scans with two schemes: the mean energy of the signal differences comparison as well as the DMAS.

REFERENCES

[1] American Cancer Society, "Cancer Statistics Center", 2018, [Online], Available: https://cancerstatisticscenter.cancer.org/#!/cancer-site/Breast. [Accessed 08. January 2020].

[2] N. Nikolova, "Microwave Imaging for Breast Cancer", *IEEE Microw. Mag.*, vol. 12, no. 7, p. 78-94, 2011.

[3] E. C. Fear et al., "Microwave Breast Imaging with a Monostatic Radar-Based System: A Study of Application to Patients", *IEEE Trans. Microw. Theory Techn.*, vol. 61, no. 5, pp. 2119-2128, 2013.

[4] M. Klemm et al., "Experimental and Clinical Results of Breast Cancer Detection Using UWB Microwave Radar"; *Proc. Antennas Prop. Soc. Int. Symp. (AP-S 2008)*, San Diego, CA, USA, Jul. 5-11, 2008.

[5] L. Kranold et al., "Clinical Study with a Time-Domain Microwave Breast Monitor: Analysis of the System Response and Patient Attributes", *Proc. 13th European Conf. on Antennas and Propagation (EUCAP2019),* Krakow, Poland, Mar 31 – Apr 5, 2019.

[6] H. Bahramiabarghouei et al., "Flexible 16 Antenna Array for Microwave Breast Cancer Detection,"in *IEEE Trans. Biomed. Eng.*, vol. 62, no. 10, pp. 2516-2525, Oct. 2015

[7] J. Garrett, "Average dielectric property analysis of non-uniform structures: Tissue phantom development, ultra-wideband transmission measurements, and signal processing techniques", *Master's Thesis*, University of Calgary, Calgary, Canada, 2014.

[8] H. Been Lim et al., , "Confocal Microwave Imaging for Breast Cancer Detection: Delay-Multiply-and- Sum Image Reconstruction Algorithm,"in *IEEE Transactions on Biomedical Engineering*, vol. 55, no. 6, pp. 1697-1704, June 2008.